LONG-PULSE, HIGH-POWER, PHASE-LOCKED MAGNETRON STUDIES*

Todd A. Treado, Paul D. Brown,
Richard A. Bolton, and Todd Hansen

Varian Associates
Crossed Field & Receiver Protector Products
150 Sohier Road
Beverly, MA 01915

ABSTRACT

We have developed a 60 MW, 60% efficient, 35 Joule/pulse secondary emission magnetron at S-band. We report on experimental results from this moderate voltage (120 kV), repetitively pulsed (10 Hz), injection locked (14-15 dB gain) magnetron. Limitations imposed by high voltage breakdown, rf breakdown, and thermal loading are discussed. By increasing the voltage, the drive power, and the magnetron length and by using a tungsten alloy anode, 120 MW should be achievable for approximately 4 μs pulses at 130 kV with the pulse length limited by transient heating of the anode.

INTRODUCTION

Two fundamentally different approaches have been followed in the development of fixed frequency high power microwave (HPM) sources. The more common approach has been the development of very large and very high power sources which typically emit Gigawatt power levels for tens to a few hundred nanoseconds and which operate in the megavolt voltage range.

The second approach is to use phase-locked arrays of more modest power level, lower voltage microwave sources which can operate for microsecond pulse lengths or longer. Examples include the split cavity oscillator and secondary emission crossed-field devices, that is, magnetrons and crossed-field amplifiers.

Conventional microwave crossed-field devices have operated in S-band at high power and energy levels (45 MW, >100 J), [1]. In addition, magnetrons can be readily phase locked and power-combined without the use of ferrite circulators [2]. The combination of high efficiency and low voltage leads to a drastic reduction in the size and weight of power conditioning equipment over HPM transmitters which utilize high voltage, low efficiency sources. This is the primary motivation for our effort to develop an HPM transmitter utilizing a secondary emission magnetron array. Other advantages of such an approach include high reliability, long life, and high repetition rate.

*This work was supported by US Army Harry Diamond Laboratory under Contract DAAL-02-89-C-0109.

EXPERIMENTAL ARRANGEMENT

The VMS-1873 magnetron has a 14-vane rising-sun anode, a secondary emission dispenser cathode, a $\lambda/2$-long copper anode and three waveguide outputs with ceramic windows.

The use of three waveguide outputs helped to reduce the loading asymmetry and resultant distortion of the π-mode electric fields. In addition, the power per waveguide was reduced to levels which could be comfortably handled by a single window.

The magnetron was injection locked to a 3 MW coaxial magnetron. Isolation was provided by two waveguide 4-port circulators pressurized with SF_6. A thyratron-switched line type modulator was used to power the high voltage magnetron. The modulator power supply limited the repetition rate to 10 Hz at 120 kV. The magnetic field was provided by a dc electromagnet which was adjustable to 4 kG. More detailed descriptions of the magnetron design, the magnetron experiment and computer simulations, and the experiment diagnostics are included in References 2 and 3.

EXPERIMENTAL RESULTS - VMS-1873 MAGNETRON

The magnetron was aged for 10^7 shots until a maximum power level of 60 MW was emitted at 2.845 GHz at a gain of 15 dB. Figures 1a-1f contain typical data taken with the magnetron operating at the 52 MW level. The horizontal time scales are synchronized in all of these plots.

Current and voltage are shown in Figures 1a and 1b, respectively. For the Figure 1 data, the Buneman-Hartree threshold voltage for the π-mode was calculated to be 97 kV. The fluctuations in the voltage pulse which begin at about 1.20 μs correspond with the magnetron oscillating in a mode other than the π-mode.

The total microwave power waveform shown in Figure 1c is a computational summation of the power waveforms emitted from each of the three loaded vanes. The 3 MW plateau before and after the pulse is not an accurate representation of the drive signal level and is due to dynamic range limitations in the diagnostics. The 2 MW drive signal is on from 0.2 μs to 2.0 μs.

The efficiency is plotted as a function of time in Fig-

gure 1d. The efficiency is calculated by dividing the total microwave power waveform by the product of the voltage and current. The microwave energy (Figure 1e) is derived by integrating the total power waveform. By measuring the energy only during the HPM magnetron pulse, from 0.55 μs to 1.40 μs, the energy per pulse is found to be 30 Joules.

The HPM magnetron was operated as an injection-locked oscillator. Figure 1f is a plot of the phase of the HPM magnetron referenced to the driver magnetron phase. While coherent from pulse-to-pulse, the magnetron phase varied during this pulse. For the Figure 1 data, the driver frequency was 14 MHz below the HPM magnetron's free running frequency and 3 MHz outside of the lock in bandwidth given by Adler's inequality [4]. Phase-locked behavior was observed when operating within the lock-in bandwith.

The maximum power level was gain limited to 60 MW at 15 dB. At 15 dB gain and independent of the power level, the magnetron oscillated unstably with changes in the frequency of oscillation occurring at the tail end of the pulse. Collapse of the current midway through the pulse was also observed at high gain.

LIMITATIONS TO THE VMS-1873 MAGNETRON DESIGN

Higher power operation of the VMS-1873 magnetron was predicted in simulations performed by Ken Eppley of SLAC (described in Reference 3). At 130 kV, 75 MW should be emitted from the $\lambda/2$-long VMS-1873 magnetron. Extending the magnetron length to 0.8 λ should result in 120 MW at 130 kV. Rising sun magnetrons have been built up to 0.8 λ long.

High voltage breakdown should not be the limiting factor in operation of the VMS-1873 magnetron at 130 kV. Estimates for the limits imposed by high voltage breakdown can be made based upon our results as well as results reported by others. Table 1 lists high voltage breakdown data applicable to the HPM magnetron. While breakdown occurs in the electron gun of a 330 kV klystron at 300 kV/cm [5], the perpendicular magnetic field of a crossed-field device such as a magnetron inhibits breakdown via magnetic insulation. For example, within one of Varian's S-band production magnetrons the maximum electric field is 440 kV/cm on the surface of the cathode end hat.

Not all high voltage breakdown mechanisms are field dependent. Microparticle-induced breakdown is also dependent upon the voltage. Therefore, most accurate comparisons are made at comparable voltages, electrode gap separations, and with comparable electrode materials, processing, and conditioning techniques. At 120 kV, the maximum surface electric field within the VMS-1873 #3 magnetron was 290 kV/cm. Occasional breakdown was observed within this tube. By modifying the end hat geometry somewhat in the VMS-1873 #4 magnetron, the maximum surface field within the VMS-1873 #4 magnetron was reduced by 20% and high voltage breakdown was virtually eliminated.

Estimates for the limits imposed by rf breakdown can also be made based upon our results as well as results reported by others. CONDOR was used to calculate the maximum rf electric field at the VMS-1873 magnetron vane tips [3]. At 120 kV, 2.1 kG, and 60 MW from the VMS-1873 magnetron, the maximum macroscopic rf electric field was calculated to be 340 kV/cm. This is almost an order of magnitude below the maximum rf field, E_s = 3100-3400 kV/cm for 1.5μs, which has been achieved within properly conditioned room temperature copper structures with a field enhancement factor of 60 [6]. Table 2 contains microsecond rf breakdown data at S-band applicable to the HPM magnetron.

The rf electric field within the magnetron is proportional to the square root of the microwave power. The rf electric field is proportional to the square root of the external Q. Loew and Wang have found empirically that the maximum surface electric field at which breakdown occurs, E_s, is proportional to the square root of the frequency [6]. Vlieks found in high power klystrons that E_s is inversely proportional to the pulse length to the one third power [5]. These relationships, listed at the bottom of Table 2, can be used (advisedly) to estimate the limits imposed by rf breakdown. The VMS-1873 magnetron would be rf-breakdown-limited to a pulse length of 30μsec at the 60 MW level and to 375 MW at a pulse length of 1.5μsec. These estimates assume that the microscopic field enhancement factor within the magnetron is 240, a value typical of what was measured from dc Fowler-Nordheim field emission data taken with a conditioned HPM magnetron.

Transient heating ($\triangle$T) of the anode will limit the peak power and the pulse length. The limitations caused by transient heating are dependent upon electrode material. We used CONDOR to calculate the average cathode and anode dissipation densities assuming that all the electrons impinge upon the vane faces opposite the cathode. To account for nonuniform dissipation across the vane tips in both the axial and the azimuthal directions, the peak dissipation density was assumed to be two times the average value. At 130 kV and 75 MW out of the $\lambda/2$-long VMS-1873 magnetron, the peak dissipation density is about 2 MW/cm^2.

Several criterion have been used in the past to limit $\triangle$T in high power tubes. These include (1) the temperature at which the thermal stresses exceed the material tensile strength, (2) the temperature at which the metal recrystallizes and loses its strength, and (3) the temperature at which the vapor pressure exceeds 10^{-8} Torr. In practice, for copper and molybdenum on the microsecond pulse length scale, criterion (1) is too conservative and criterion (3) is too liberal.

Table 3 lists the time to reach the temperature limits imposed by thermal stress, recrystallization, and outgassing at 2 MW/cm^2 incident electron beam density and 40 keV electron energy. According to Table 3, the pulse

length is limited by a 2200°C transient temperature rise at about 4μs for a 75 MW pulse from the $\lambda/2$-long VMS-1873 magnetron with a tungsten-rhenium-hafnium-carbide anode. Tungsten-rhenium alloys have very high strength at elevated temperatures and should be less susceptible to mechanical stress from cyclic electron bombardment than is tungsten.

FUTURE PLANS

Presently, we are attempting to determine the limits of this type of technology by performing a series of experiments with copper, molybdenum, tungsten, and tungsten alloy anodes. We are also building a two magnetron array (50 MW each) to demonstrate at high power our technique of phase locking and power combining without the use of ferrite circulators [3]. In addition, a small, lightweight permanent magnet based version of the VMS-1873 HPM magnetron will be tested this year (1992).

REFERENCES

[1] W.C. Brown and J.S. Skowron, *Ultra high power amplitron, Vol 2. Pulsed amplitron development.* Technical Report No. RADC-TDR-64-389, May 1965.

[2] T.A. Treado, et al., "High-energy, high-efficiency, phase-locked HPM magnetron for an array," in *Proceedings SPIE Intense Microwave Particle Beams III Symposium*, (Los Angeles, CA) 1992.

[3] T.A. Treado, et al., "High-power high-efficiency, secondary emission magnetron," submitted to *IEEE Trans. Plasma Science.*

[4] R. Adler, *Proc. IRE* **34**, 351 (1946).

[5] A.E. Vlieks, et al., *IEEE Trans Elect. Insul.* **24**, 1023 (1989).

[6] G.A. Loew and J.W. Wang, "Progress report on high-gradient rf studies in copper accelerator structures," in *Proc. XIVth Int. Symp. on Discharges and Electrical Insul. in Vacuum* (Santa Fe, New Mexico), 1990.

[7] R.V. Latham, *High Voltage Vacuum Insulation: The Physical Basis.* London: Academic Press, 1981.

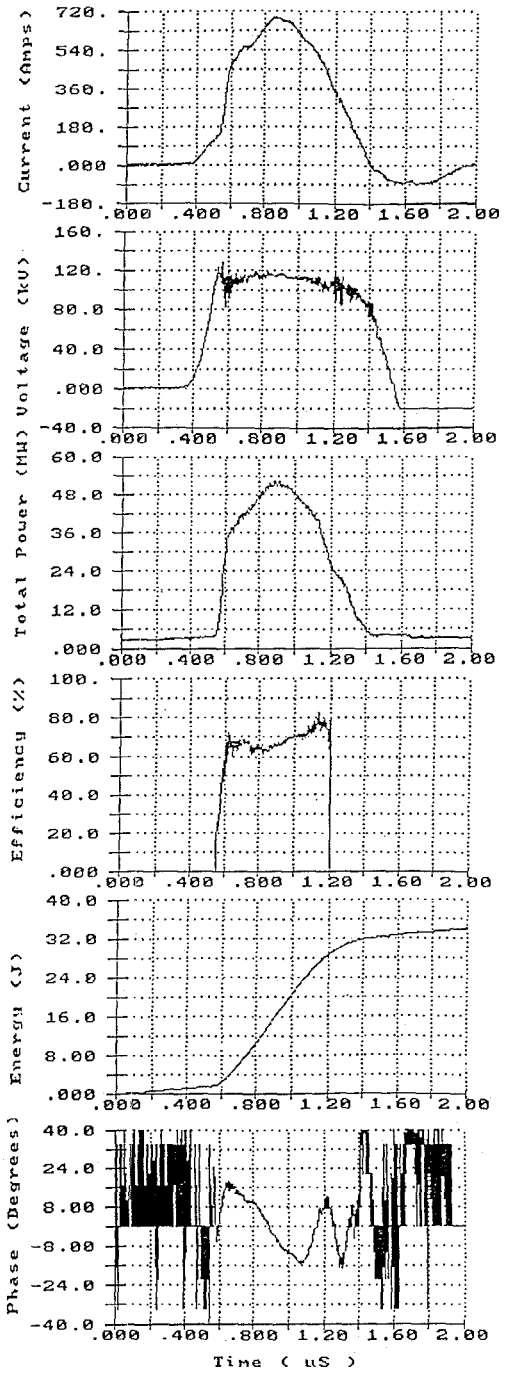

Figure 1. Typical data for B = 2.1 kG. (a) Current, (b) Voltage, (c) Total microwave power coupled out of three waveguides, (d) Efficiency, (e) Microwave energy, (f) Phase referenced to driver.

TABLE 1 - Microsecond H.V. Breakdown

Application	Electric Field (kV/cm)	Voltage (kV)	Pulse Length (μs)	Magnetic Field Orientation	Break-down	Author
Microscopic	60,000-70,000	–	DC	None	Yes	Latham [7]
Klystron E Gun	300	330	3.3	Parallel	Yes	Vlieks et al [5]
Magnetron	440	68	2.2	Perpendicular	No	Varian
VMS-1873 #3 Magnetron	290	120	0.6	Perpendicular	Occasionally	Treado et al [3]
VMS-1873 #4 Magnetron	220	110	0.6	Perpendicular	No	Treado et al [3]

TABLE 2 - Microsecond rf Breakdown at S-band

Application	Maximum Surface RF Electric Field (kV/cm)	RF Power (MW)	Pulse Length (μS)	Break-down	Author
Accelerator Cavities (Copper, Room Temp)	3100-3400 ($\beta = 60$)	–	1.5-2.5	Yes	Loew & Wang [6]
Klystron Output Gap	440	100	2	No	Vlieks, et al. [5]
	360	67	3.5	No	
VMS-1873 Magnetron Resonator Opening	340	60	0.6	No	Treado, et al., [3]

$E_s \alpha P^{1/2}$, $E_s \alpha Q_E^{1/2}$,
$E_s \alpha f^{1/2}$, Loew & Wang, [6]
$E_s \alpha 1/\tau^{1/3}$, Vlieks, et al., [5]

TABLE 3 - Transient Heating

Material	Time to Reach Tensile Strength Limit (μs)	Time to Reach Recrystallization Temperature (μs)	Time to Reach Vapor Pressure Limit (μs)
Cu	0.13	0.15-0.45	2.1
Mo	0.3	1.8	2.7
Mo 50 Re	0.4	0.6-0.8	
TZM Mo	0.5	2.0	
Re	0.24	0.7-0.8	1.5
W	0.9	2.6	4.3
W 25 Re	0.7	1.6-1.9	
W 4 Re 0.35 HfC	1.6	4.4	4.3

P_A = 2 MW/cm^2 (Factor of 2 included for nonuniform dissipation)
E_A = 40 KeV
R_{RF} = 60 MW
60% Efficiency